Development and Evaluation of an Integrated Chassis Control System

Youseok Kou[1]

Huei Peng[2]

DoHyun Jung[3]

1 Graduate Student, Dept. of Mechanical Engineering, University of Michigan, Ann Arbor, MI 48109 USA

2Professor, Dept. of Mechanical Engineering, University of Michigan, Ann Arbor, MI 48109 USA

3Senior Researcher, Body & Chassis Engineering Center, Korea Automotive Technology Institute, South Korea

Abstract

The development and worst-case evaluation of an Integrated Chassis Control (ICC) system is reported in this paper. The ICC control system was designed based on a lateral-yaw-roll vehicle model with nonlinear tires. The ICC controller was developed based on balanced objectives in controlling vehicle motions, with carefully selected thresholds and targets. The sliding mode control technique is used to design the brake torque servo loop to achieve the desired outputs. Vehicle response under the ICC control

is evaluated using the CarSim software. The effectiveness of the ICC system was examined by applying the worst-case dynamic evaluation (WCDE) procedure, which identifies the worst-possible excitation (e.g., steering) to the vehicle with ICC and thus represents a procedure suitable for the evaluation of active safety systems.

1. INTORDUCTION

The general public and government agencies have demonstrated sustained interest in active safety technology for ground vehicles. Many chassis control devices that manipulate braking, steering and suspension systems were developed and applied to improve vehicle safety, conveniences and comfort. As these devices become more mature, they need to share information with each other for better cost-leveraging and improved reliability and performance. The integration of these chassis control functions is loosely referred to as Integrated Chassis Control systems, and has been an area of intensive development by many companies in recent years (1). Major automotive companies have developed a wide array of chassis control functions, many of which are already commercialized (2).

A critical issue of these active safety systems is to ensure their functionality under extreme circumstances.

Typically, large-scale test matrices were defined and the active safety systems were evaluated using these test matrices iteratively. To avoid time-consuming field testing, computer simulations can be used to systematically search for worst-cases situations, i.e., potential cases when the active safety systems might fail to perform satisfactorily. The worst-case dynamic evaluation (WCDE) methodology is an emerging field which has the potential to accelerate the development of vehicle active safety systems (3), by replacing lengthy field tests and calibration with elaborative numerical simulations.

Vehicle models suitable for ICC design and evaluation must be accurate enough under extreme maneuvers and in the meantime easy to be integrated with ICC controller and possibly other software wrappers. Because ICC systems operate under near-incident conditions, the accuracy of the model under severe maneuvers is crucial.

The vehicle model developed in this paper is a 3 DOF (yaw, roll, lateral) vehicle dynamic model with a nonlinear tire sub-model. The model is verified against the CarSim software, which has 16 DOF and comprehensive nonlinear tire and suspension modules. It is assumed that the Carsim model output represents the true vehicle response up to wheel lift-off and will be used to assess the accuracy of the

3DOF model.

In the ICC design, we focus on the integration of a differential braking function (Electric Stability Program, ESC) and a suspension function (Continuous Damping Control, CDC). This relatively simple ICC configuration makes it easier to study the integration and interaction of the vehicle control functions. The functional characteristics of the sub-systems are categorized by ride comfort, lateral stability, side-slip control, yaw control, rollover prevention and wheel slip control. The ICC control was designed at two levels. At the upper level, the desired suspension damping and brake torques are calculated based on yaw, side slip, roll and ride considerations. The servo control for the braking control is realized based on a sliding mode control technology, which is modified slightly to avoid the complex nonlinear form(4). The braking forces are obtained by using the tire ellipse concept (5). This ICC system is intended to emulate the typical functions of a production ICC, and is designed to be modular so that additional control systems can be added. This model will be used in our simulation based worst-case study and could be integrated in HILS system with the ICC part implemented in hardware(6). The worst-case evaluations, HIL test, and road test are future tasks of our research that are not reported in this paper.

The remainder of this paper is as follows. In Section 2, a lateral yaw roll model is developed, which is critical for the ICC control development. In Section 3, the ICC system design is described. In Section 4, standard tests and WCDE procedure for vehicle rollover is discussed. In Section 5, the performance of ICC rollover prevention is evaluated via simulations based on both standard tests and WCDE. A conclusion section is included at Section 6.

2. VEHICLE MODEL

A simple vehicle model is developed to describe vehicle handling and roll behavior, which includes the lateral, roll and yaw motions as shown in Eq.(1)

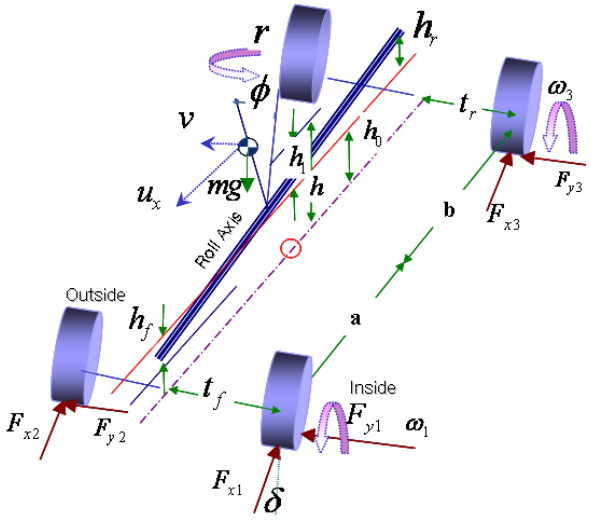

Fig. 1 Vehicle model

$$mh_1\dot{v} + I_{xx}\dot{p} + mh_1u_x r = L_\phi \phi + L_p p + h_{cf}\sum_{i=1}^{2} F_{yi} + h_{cr}\sum_{i=3}^{4} F_{yi}$$

$$I_{zz}\dot{r} = a\sum_{i=1}^{2} F_{yi} - b\sum_{i=3}^{4} F_{yi} - t_f F_{x1} - t_r F_{x3} + t_f F_{x2} + t_r F_{x4}$$

$$m\dot{v} + mh_1\dot{p} + mu_x r = h_f \sum_{i=1}^{2} F_{yi} + h_r \sum_{i=3}^{4} F_{yi} \qquad \text{Eq.(1)}$$

where $p = \dot{\phi}, L_\phi = mgh - K_R, L_p = -C_R, i = 1,2,3,4$. K_R is the roll stiffness and C_R is the roll damping coefficient.

The variables and parameters all follow the SAE standard as shown in Fig. 1. Eq.(1) can be written in the state space form. For this 3DOF system, 4 state variables are needed. The state space model is

$$M_1\dot{X} = M_{2m}X + M_y F_y + M_x F_x \qquad \text{Eq.(2)}$$

where

$$X = \begin{bmatrix} r & v & \phi & p \end{bmatrix}^T \qquad \text{Eq.(3)}$$

$$F_y = \begin{bmatrix} F_{y1} & F_{y2} & F_{y3} & F_{y4} \end{bmatrix}^T$$
$$F_x = \begin{bmatrix} F_{x1} & F_{x2} & F_{x3} & F_{x4} \end{bmatrix}^T \qquad \text{Eq.(4)}$$

$$M_1 = \begin{bmatrix} 0 & m & 0 & mh_1 \\ 0 & mh_1 & 0 & I_{xx} \\ I_{zz} & 0 & 0 & \varepsilon I_{zz} \\ 0 & 0 & 1 & 0 \end{bmatrix}, M_{2m} = \begin{bmatrix} -mu_x & 0 & 0 & 0 \\ -mh_1u_x & 0 & L_\phi & L_p \\ 0 & 0 & 0 & 0 \\ 0 & 0 & 0 & 1 \end{bmatrix} \qquad \text{Eq.(5)}$$

$$M_x = \begin{bmatrix} 0 & 0 & 0 & 0 \\ 0 & 0 & 0 & 0 \\ -t_f & t_f & -t_r & t_r \\ 0 & 0 & 0 & 0 \end{bmatrix}, M_y = \begin{bmatrix} 1 & 1 & 1 & 1 \\ h_f & h_f & h_r & h_r \\ a & a & -b & -b \\ 0 & 0 & 0 & 0 \end{bmatrix} \qquad \text{Eq.(6)}$$

The tire forces shown in Fig.2 are calculated from the tire force equations:

$$J_w\dot{\omega}_j = -T_b + r_w F_{xj} \qquad \text{Eq.(7)}$$

$$\lambda_j = \frac{u_x - r_w \omega_j}{u_x},\ j = 1,2,3,4 \qquad \text{Eq.(8)}$$

The wheel slip, λ_i in Eq.(8) determines the tire longitudinal force and is used for wheel slip control. In our tire model, tire longitudinal forces and the lateral force are calculated via the tire ellipse concept:

$$F_{yj} = F_{y\max}(\alpha, F_{zj})\sqrt{1-\left(\frac{F_{xj}}{\mu F_{zj}}\right)^2} \qquad \text{Eq.(9)}$$

where T_b is the braking torque, J_w is the angular moment inertia of the wheel, α is the slip angle, μ is road friction coefficient, and r_w is the wheel radius.

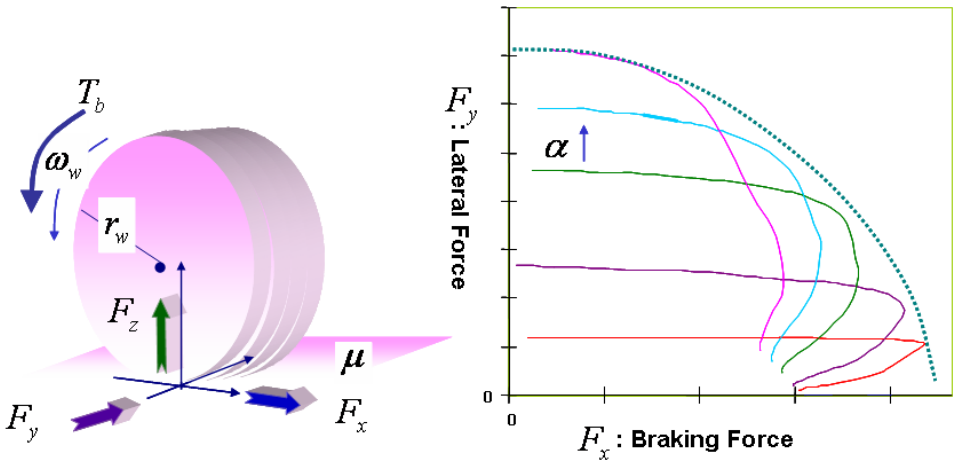

Fig. 2 Wheel model & Ellipse of tire

For the above equations, the inputs for the body motion are the tire forces and those for the wheel motions are the braking torques. Lateral tire forces and longitudinal tire force are related through the friction ellipse Eq.(9). The tire model consists of 3 major

components, which calculate tire vertical forces, slip angles, and the tire relaxation length. In this paper, we use look-up tables identical to those used in the CarSim software.

The vehicle model is written in MATLAB based on Eq. (1)-(9). It has four major sub-systems for vehicle lateral/yaw/roll dynamics, longitudinal velocity, wheel dynamics, and tire force computations. In the vehicle state space block, the vehicle model is processed linearly using the tire forces and the vehicle longitudinal velocity. In addition to the 4 state variables shown in Eq.(3), longitudinal velocity is another important variable, which is assumed to be slow-varying in the linear lateral/yaw/roll model computation. The longitudinal velocity and the wheel speeds are calculated separately based on tire forces and wheel rotational dynamics. Since these dynamic variables are included, the performance of brake control systems such as ABS and ESC can be included and evaluated.

It should be noted that even though we refer to the model presented above as a 3DOF model, which reflects the major dynamic captured, it is somewhat misleading. In reality, we also simulate vehicle forward speed and the wheel speeds, and thus the overall DOF is 8, instead of 3.

The developed model is verified by comparing its simulation results against those of the CarSim software.

We performed a large number of simulations, with frequent rollover, spin out and plow out.

The target vehicle in this paper is an SUV, which has a higher center of gravity (C.G). To match the response from the two models, we need to carefully adjust the tire cornering stiffness, sprung mass height h_f, h_r and suspension roll stiffness and damping rate.

Fig. 3 shows the difference between the responses from the two models, measured in infinity-norm. The difference in the vehicle lateral speed is as large as 20%. This difference may cause some discrepancies in the ICC system response when the vehicle side slip angle is used in the control decision.

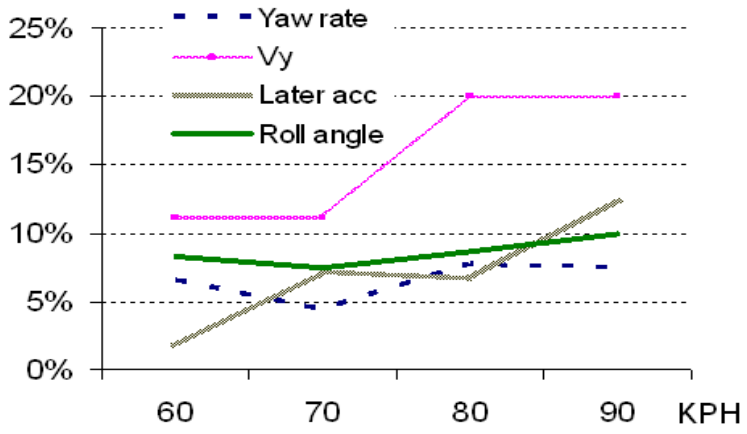

Fig. 3 $\|e\|_\infty$, difference between CarSim and the 3DOF model under step steer of 100 degrees.

3. ICC SYSTEM DESIGN

The ICC system studied in this paper consists of a Continuous Damping Control (CDC) system, and an

Electronic Stability Control (ESC) system. The CDC system manipulates suspension damping based on two considerations: lateral motion control and vertical vibration suppression. The ESC system adjusts hydraulic pressure at the brake cylinder of four wheels independently to assist vehicle lateral, yaw and roll motion. These two control functions will be explained in the following sections.

3.1 CDC System

The Continuous Damping Control system controls the sprung mass motion by changing the setting of the variable damper using a solenoid valve. The control algorithm uses information such as vertical acceleration and velocity, and steering input to manifest the behavior of the vehicle and the intention of the driver.

Ride control is based on Skyhook damping concept, which uses a desired damping force that is proportional to the vertical velocity of the sprung mass (39). Kinetic energy of the sprung mass is dissipated by the imagined sky-hook damper which ensures decaying energy content and thus improved ride quality for the occupants. The sky-hook damper is realized through the variable suspension dampers of CDC system.

The sprung mass vertical velocities at the four corners necessary for realizing the skyhook damping strategy are

calculated from the corner acceleration sensors through band-pass filtered integrators. Ride control of the developed CDC is based on damping of vehicle motions in three directions: heave, pitch and roll, which are calculated from

$$\dot{z}_{\text{heave}} = \sum_{i=1}^{4} \dot{z}_i, \dot{z}_{\text{ptch}} = \sum_{i=1}^{2} \dot{z}_i - \sum_{i=3}^{4} \dot{z}_i, \ \dot{z}_{\text{roll}} = \sum_{i=1}^{4} (-1)^i \dot{z}_i \qquad \text{Eq.(10)}$$

The control gains, $K_{\text{ride}}^{\text{heave}}, K_{\text{ride}}^{\text{pitch}}, K_{\text{ride}}^{\text{roll}}$ for each control mode are adaptively calibrated according to vehicle speed and then the desired damping forces corresponding to each mode are calculated as $F_l^{\text{CDC}} = K_{\text{ride}}^{l} \cdot \dot{z}_l, where \ l = \text{heave,pitch,roll}$. The averaged desired damping forces are finally distributed to each axles in accordance with the ride control gain of each corner, K_{ride}^{i} where $i = 1 \sim 4$.

Lateral stability control of CDC aims to stabilize vehicle motion resulted from driver's steering during high speed cornering. The activation of lateral stability control is decided based on vehicle lateral acceleration, estimated from the bicycle model:

$$\hat{a}_y = \delta \cdot u_x^2 \cdot \left(1 + \left(u_x / u_{ch}\right)^2\right)^{-1} \frac{1}{L} \qquad \text{Eq.(11)}$$

This estimated acceleration is a better signal to use than that from an accelerometer because of its predictive nature and because it is less vulnerable to road grade and cross-talk disturbances. The quality of the estimation

provided by Eq.(11) depends on the accuracy of our estimate of characteristic speed, which depends on tire cornering stiffness. The gain scheduling process for lateral stability control follows a similar process executed in the ride control. Lateral stability control gains, K_{lat} is adaptively calibrated according to vehicle speed and then the desired damping torque which is calculated as $T_{\text{lat}}^{\text{CDC}} = K_{lat} \cdot \hat{a}_y$ are distributed through final gains allocation.

The overall procedure of the CDC algorithm is described in the flow chart in Fig. 5. A desired force is calculated from both the lateral stability and ride control parts. The lateral stability takes priority over ride control when the estimated lateral acceleration is higher than a speed-dependent safety threshold value.

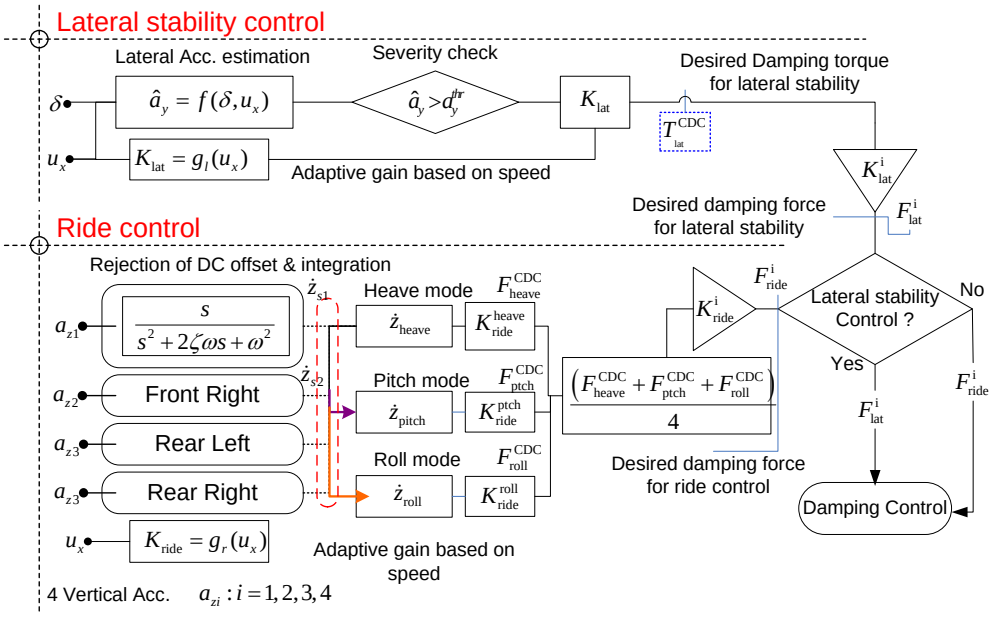

Fig. 4 Flow chart of the CDC algorithm

3.2 ESC System

The ESC system controls the braking forces of the four tires to stabilize vehicle roll and yaw motions. Based on Eq.(1)-(9), we obtain a vehicle model of four states. Adding the wheel speeds, an eight-state model is used for our control synthesis. In the following we will define the major functions of the ESC system and the target state values. The general ESC system (which includes the ABS functions) includes four control objectives. In the order of descending priority, these four functions are: wheel slip control, rollover prevention control, yaw control and side slip control. The wheel slip control is imposed to limit magnitude of the wheel slip to be below

0.1. The other three control functions are active when threshold values are exceeded (roll and side slip) or when the error is large (yaw). A desired yaw rate is calculated first from linear vehicle steady-state cornering:

$$r_d = \frac{\delta \cdot u_x}{1+\left(u_x / u_{ch}\right)^2} \cdot \frac{1}{L} \qquad \text{Eq.(12)}$$

This value is then saturated based on a nominal road friction value and vehicle forward speed

$$\left|r_d\right| \le r_{\lim} = \left|\frac{\mu \cdot g}{u_x}\right| = \left|\frac{a_y}{u_x}\right| \qquad \text{Eq.(13)}$$

The obtained desired yaw rate is used to calculate a yaw error, $\Delta r = r_d - r_m$ where r_m measured yaw rate, based on which a yaw control command will be calculated.

The limit for the side slip angle, λ_{thresh} is chosen to be 5 degrees. When this threshold value is exceeded, yaw moment will be requested to reduce the magnitude of the side slip angle to maintain driver's control authority.

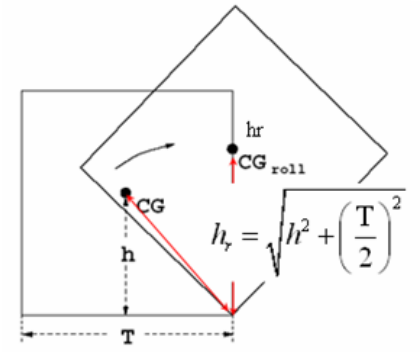

Fig. 5 Analysis of rollover dynamics

Fig. 5 shows the change of geometry characteristics

based on Center of Gravity (C.G) point during a rollover of ground vehicle. The rollover threat is measured by the total amount of energy stored in the vehicle—including both potential energy and kinetic energy. Assuming that K_s is the suspension roll stiffness and ϕ_c is the roll angle, the vehicle critical roll rate, beyond which enough kinetic energy exists to roll over the vehicle, can be calculated from

$$\dot{\phi}_c = \frac{mg\left(\sqrt{4h^2 + T^2} - 2h\right)}{I_{xx}} = \frac{2mg(h_c - h_0)}{I_{xx}} + \frac{K_s \phi_c^{\,2}}{I_{xx}} \qquad \text{Eq.(14)}$$

To improve the responsiveness of the control system, predicted vehicle roll rate, instead of measured vehicle roll rate, is used. The predicted roll rate is calculated from

$$\begin{aligned} \dot{\phi}_p(t) &= \dot{\phi}(t+\tau) = \dot{\phi}(t) + \ddot{\phi} \cdot \tau \\ &= \dot{\phi}(t) + \left(-\frac{k_\phi \cdot \phi(t) + b_\phi \cdot \dot{\phi}(t)}{I_{xx}} + \frac{m h_{Rc}}{I_{xx}} \cdot a_y \right) \cdot \tau \end{aligned} \qquad \text{Eq.(15)}$$

where t is the present time and τ is the prediction time. The roll rate is predicted based on roll rate at the present time and the roll acceleration. The roll acceleration information is estimated from a simple roll dynamic model.

The ESC control logic is shown in Figure 6. The desirable yaw rate is first inferred from steering input and forward speed, which is saturated according to Eq.(13). In parallel, the side slip threshold, 5[deg] and the critical roll rate of the vehicle are derived. The differences

between yaw rate, side slip and roll rate and their threshold values are then calculated. If the difference is larger than a threshold gap, $\Delta\beta_{thr}, \Delta r_{thr}, \Delta\dot{\phi}_{thr}$, the corresponding control module is turned on. Based on the priorities of the four control objectives, the corresponding servo controllers in Section 3.3 are checked to see whether they should be activated. The desirable brake force obtained from the servo controller is passed onto the brake system. The controller detects the vehicle turning direction based on the direction of the lateral acceleration to select the wheels to be braked. The brake force is finally regulated by wheel slip control to prevent wheel lock-up, which is based on ABS system.

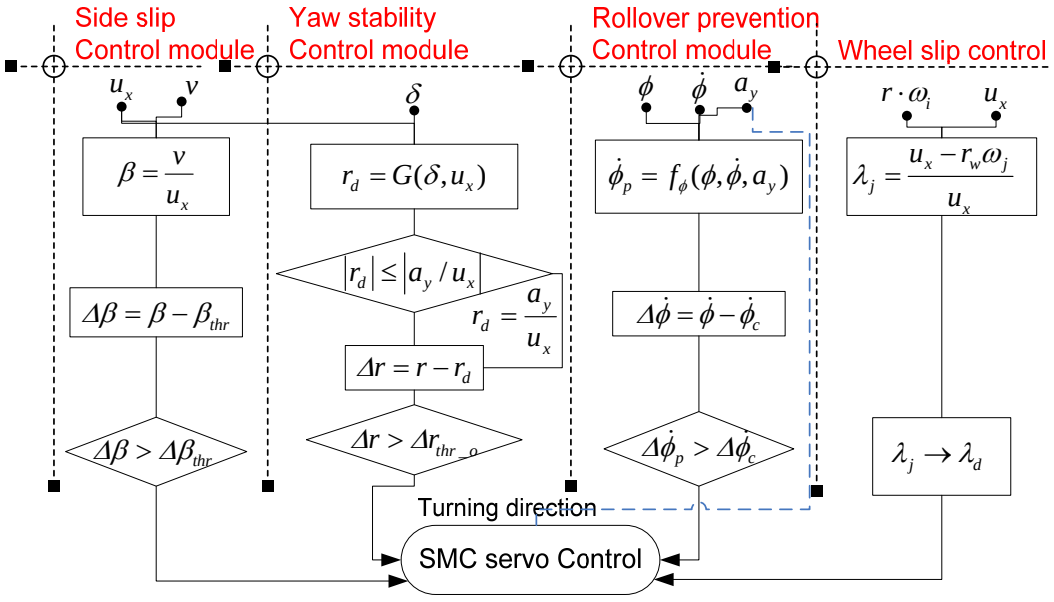

Fig. 6 Flow chart of the ESC control algorithm

Before the CDC and ESC control command can be sent to

the servo loop, an ICC master needs to determine the final control command based on prioritized control objectives. The ESC control command will take priority over that of CDC and the respective control system is operated in its priority sequence as explained above. Network between ride control of CDC and rollover prevention control of ESC enables two modules to share the information about vehicle roll motion. Networks of various control information for performance improvement and fault tolerance system are also possible. Integration strategy in this paper is based on organizing the control elements in priority sequence as shown in Fig. 8.

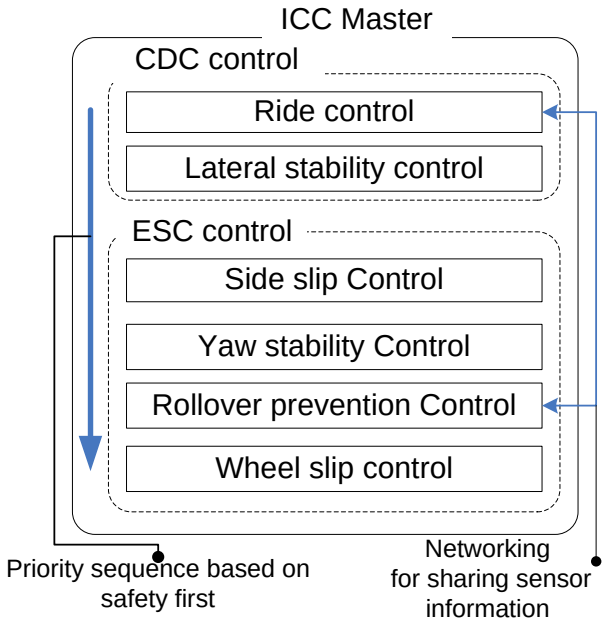

Fig. 7 ICC master strategy

3.3 Sliding Mode Control (SMC) Strategy

In the previous two sections, we presented the CDC and ESC algorithms. In this section, we will present a sliding mode control algorithm, which calculates the braking torque to achieve the desired slip ratios and other desired vehicle state. The CDC control is achieved through servo valves and does not need additional servo-control algorithms. However the ESC controller needs the additional servo-control algorithm such as the robust control to overcome the parametric uncertainties and un-modeled dynamics.

In this paper we use SMC as the servo-control because of its robustness. Chattering, which is sometimes a concern for practical implementations, is nothing uncommon for brake control. To apply the SMC algorithm, we first re-compose the linear vehicle model where the braking force F_x is defined as the control input. This linear model enables us to avoid complexity and difficulty found in the nonlinear tire model-based SMC design, where nonlinear observer-based design such as extended Kalman filters and sliding observers may be necessary. Using this linear model, the nonlinearities such as tire friction ellipse will be lumped to the uncertainty term, which will be addressed by the high-gain switching.

The simple vehicle model derived earlier in Eq.(2) will now be rewritten with steering angle as the

disturbance input.

$$\dot{X} = M_1^{-1}M_2X + M_1^{-1}M_3\delta = AX + B_\delta\delta \qquad \text{Eq.(16)}$$

where δ is tire steering angle, M_1 is given in Eq. (3), and M_2 and M_3 are defined as follows

$$M_2 = \begin{bmatrix} \frac{-aC_{\alpha f}+bC_{\alpha r}}{u_x} - mu_x & -\frac{C_{\alpha f}+C_{\alpha r}}{u_x} & Cy_{R\&C\phi} & 0 \\ -m_R h_1 u_x & 0 & -L_\phi + mgh_1 & -L_p \\ -\frac{a^2C_{\alpha f}+b^2C_{\alpha r}}{u_x} & \frac{-aC_{\alpha f}+bC_{\alpha r}}{u_x} & Cn_{R\&C\phi} & 0 \\ 0 & 0 & 0 & 1 \end{bmatrix} \qquad \text{Eq.(17)}$$

$$M_3 = \begin{bmatrix} C_{\alpha f} & 0 & aC_{\alpha f} & 0 \end{bmatrix}^T \qquad \text{Eq.(18)}$$

where $C_{\alpha f}$, $C_{\alpha r}$: Cornering stiffness, $Cy_{R\&C\phi}$, $Cn_{R\&C\phi}$: Roll steer factor, L_ϕ, L_p: roll stiffness and damping coefficient. Eq.(16) is idealized without any plant uncertainties and no control input. It can be rewritten as

$$M_1\dot{X} = M_2X + M_3\delta \qquad \text{Eq.(19)}$$

where F_y^0 is the pure-slip lateral tire force. With F_x input, Eq.(19) becomes

$$\dot{X} = AX + B_\delta\delta + BF_x + F \qquad \text{Eq.(20)}$$

where the model uncertainty, F and the matrix B are derived in the following.

The overall tire input U is defined as

$$U = M_xF_x + M_yF_y \qquad \text{Eq.(21)}$$

The truncated Taylor's series at the operating point is

$$M_x F_x + M_y F_y = M_x F_x + M_y \left(F_{y0} + \frac{\partial F_y}{\partial F_x}(F_x - F_{x0}) \right) \qquad \text{Eq.(22)}$$

$$U + M_y \left(\frac{\partial F_y}{\partial F_x} \cdot F_{x0} - F_{y0} \right) \approx \left(M_x + M_y \frac{\partial F_y}{\partial F_x} \right) F_x$$
$$B = M_1^{-1} \left(M_x + M_y \frac{\partial F_y}{\partial F_x} \right) \qquad \text{Eq.(23)}$$

where F_{x0}, F_{y0}: The tire forces of the operating point, where braking force is generated

$$\frac{\partial F_{y0}}{\partial F_x} = \begin{bmatrix} c_{l1L} & 0 & 0 & 0 \\ 0 & c_{l1R} & 0 & 0 \\ 0 & 0 & c_{l2L} & 0 \\ 0 & 0 & 0 & c_{l2R} \end{bmatrix}, \; c_{li} = \frac{-F_{xi0} F_{y\max}(\alpha_1, F_{zi})}{\mu F_{zi} \sqrt{(\mu F_{zi})^2 - F_{xi0}^2}}$$

And then the linearized tire model using Eq.(22). The lateral force F_y can be estimated from

$$M_y F_y \approx M_y \left(F_{y0} - \frac{\partial F_y}{\partial F_x} F_{x0} \right) + M_y \frac{\partial F_y}{\partial F_x} F_x \qquad \text{Eq.(24)}$$

If we eliminate the effect of F_x from the right-hand side of Eq.(24), the estimated free rolling vehicle model is

$$M_{2m} X + M_y F_y^0$$
$$\approx M_{2m} X + M_y F_y - M_y \frac{\partial F_y}{\partial F_x} F_x = M_{2m} X + M_y \left(F_{y0} - \frac{\partial F_y}{\partial F_x} F_{x0} \right) \qquad \text{Eq.(25)}$$

which can be written using Eq.(19) as

$$M_2 X + M_3 \delta \approx M_{2m} X + M_y \left(F_{y0} - \frac{\partial F_y}{\partial F_x} F_{x0} \right) \qquad \text{Eq.(26)}$$

If we insert Eq.(26) to the linearized vehicle form Eq.(27).

$$M_1\dot{X} \approx M_{2m}X + M_y\left(F_{y0} - \frac{\partial F_y}{\partial F_x}F_{x0}\right) + M_y\frac{\partial F_y}{\partial F_x}F_x + M_xF_x \qquad \text{Eq.(27)}$$

We can then get the final vehicle model

$$M_1\dot{X} = M_2X + M_3\delta + M_y\frac{\partial F_y}{\partial F_x}F_x + M_xF_x \qquad \text{Eq.(28)}$$
$$(\because M_{2m}X + M_yF_y + M_xF_x)$$

The nominal linear vehicle model is then

$$\dot{X} = AX + B_\delta\delta + BF_x \equiv f(X,t) + BF_x \qquad \text{Eq.(29)}$$

where $f(X,t)$ is unknown but can be approximated by a nominal value $\hat{f}$, the estimation error is assumed to be bounded by F, i.e., $\left|f(X,t) - \hat{f}\right| \le F$.

To achieve the control target respect to the desired yaw, side-slip, roll rate and wheel slip ratio, the brake torque at each wheel is designed from the SMC strategy. For sliding mode controls, we first define a switching surface:

$$S = \tilde{X} = X - X_d \qquad \text{Eq.(30)}$$

where X_d denotes the desired value of the state vector.

$$X_d = \begin{bmatrix} r_d & v_d & \dot{\phi}_d \end{bmatrix}^T \qquad \text{Eq.(31)}$$

The sliding surface s^i defined the element of the sliding surface vector S. Superscript, $i = N,Y,L$ represents the three control modules shown in Fig.7 (N: Yaw motion, Y: Side slip motion, L: roll motion). The sliding mode control gain is assumed to be bounded by

$$b^i_{c\min} \le b^i_c \le b^i_{c\max} \qquad \text{Eq.(32)}$$

where b_c^i is the column vector of the control gain vector B. The parameters for control gain β_i, b_c^i can be written as

$$\beta^{i-1} \le \frac{\hat{b}_c^i}{b_c^i} \le \beta_i, b_c^i = \sqrt{b_{c\min}^i b_{c\max}^i} \quad , \beta^i = \sqrt{\frac{b_{c\max}^i}{b_{c\min}^i}} \qquad \text{Eq.(33)}$$

The dynamics while in the sliding mode can be written as

$$\dot{S} = AX + B_\delta \delta + b_c u - \dot{X}_d = 0 \qquad \text{Eq.(34)}$$

To satisfy Eq.(34), the equivalent control input without model error needs to satisfy

$$b_c u_{eq} = -AX - B_\delta \delta + \dot{X}_d \qquad \text{Eq.(35)}$$

The equivalent control input u_{eq}^i are defined as the element of u_{eq} .The equivalent control input of yaw/lateral/roll motion are taken as

$$\begin{aligned} a_{Nr} r + a_{Nv} v + a_{N\phi} \phi + b_{N\delta} \delta &= -b_c^N u_{eq}^N + \dot{r}_d \\ a_{Yr} r + a_{Yv} v + a_{Y\phi} \phi + a_{Y\dot{\phi}} \dot{\phi} + b_{Y\delta} \delta &= -b_c^Y u_{eq}^Y + \dot{v}_d \\ a_{Lr} r + a_{Lv} v + a_{L\phi} \phi + a_{L\dot{\phi}} \dot{\phi} + b_{L\delta} \delta &= -b_c^L u_{eq}^L + \ddot{\phi}_d \end{aligned} \qquad \text{Eq.(36)}$$

The coefficients of Eq.(36) are given in the following.

$$a_{Nr}=-\frac{a^2C_{af}+b^2C_{ar}}{I_{zz}u_x},a_{Nv}=\frac{(-aC_{\alpha f}+bC_{\alpha r})}{I_{zz}u_x},a_{N\phi}=\frac{C_{NRC\phi}}{I_{zz}}$$

$$a_{Yr}=\frac{I_{xx}}{m\cdot D}\left(\frac{(-aC_{\alpha f}+bC_{\alpha r})}{u_x}-mu_x\right)-\frac{h_1{}^2mu_x}{D},a_{Yv}=-\frac{I_{xx}(C_{\alpha f}+C_{\alpha r})}{mu_xD},$$

$$a_{Y\phi}=-\frac{I_{xx}C_{yr\phi}}{m\cdot D}+\frac{h\left(-K_f-K_r-mgh_1\right)}{D},a_{Y\dot{\phi}}=\frac{h_1\left(-B_f-B_r\right)}{D}$$

$$a_{Lr}=\frac{h_1}{m\cdot D}\left(\frac{(-aC_{\alpha f}+bC_{\alpha r})}{u_x}-mu_x\right)-\frac{hmu_x}{D},a_{Lv}=-\frac{h_1(C_{\alpha f}+C_{\alpha r})}{u_xD},$$

$$a_{L\phi}=-\frac{h_1C_{yr\phi}}{m\cdot D}-\frac{h\left(-K_f-K_r-mgh_1\right)}{D},a_{L\dot{\phi}}=-\frac{\left(-B_f-B_r\right)}{D}$$

$$b_{N\delta}=\frac{aC_{\alpha f}}{I_{zz}},b_{Y\delta}=-\frac{I_{xx}C_{af}}{m\cdot D},b_{L\delta}=-\frac{h_1C_{af}}{D},D=mh_1^2-I_{xx}$$

The final control law which satisfies the sliding condition is (9):

$$u^i=u^i_{eq}-k^i/b^i_c\cdot isat(s^i)$$

$$with\ \ k^i\ \geq\beta^i(F^i+\eta^i)+(\beta^i-1)\left|u^i{}_{eq}\right| \qquad \text{Eq.(37)}$$

$$where\ isat(s)=\begin{cases}1 & if\ s\geq 1\\ s & if\ -1<s<1\\ -1 & if\ s\leq -1\end{cases}$$

Here, $isat(s)$ is used instead of a sign function in order to avoid chattering problem due to a switching control.

The final wheel slip control regulates the braking force, to maintain the longitudinal slip ratio zone (0.1~0.15) of maximizing the braking force. In order to realize the wheel slip control, we define a new sliding surface as

$$s^\lambda=\lambda-\lambda_d \qquad \text{Eq.(38)}$$

And the wheel dynamics along the sliding surface is

$$\dot{\lambda} - \dot{\lambda}_d = -\frac{\dot{u}_x}{u_x}(\lambda - 1) - \frac{r_w}{J_w u_x}\left(r_w F_x - T_b\right) - \dot{\lambda}_d \qquad \text{Eq.(39)}$$

The corresponding equivalent brake torque as

$$u_{eq}^{\lambda} = r_w F_x + \frac{J_w \dot{u}_x}{r_w}(\lambda - 1) \qquad \text{Eq.(40)}$$

The wheel slip control input, u_λ can be obtained in the same way in shown as Eq.(34)~Eq.(36) and it is used as the braking force based on $T_b \propto F_b \cdot r_w$.

The final control inputs forms including the body motion and the wheel motion are taken as

$$\begin{aligned} u_r &= u_{eq}^{N} - b_c^{N-1} k^{N} \cdot isat(r - r_d) \\ u_v &= u_{eq}^{Y} - b_c^{Y-1} k^{Y} \cdot isat(v - v_d) \\ u_{RI} &= u_{eq}^{L} - b_c^{L-1} k^{L} \cdot isat(\dot{\phi} - \dot{\phi}_d) \\ u_{\lambda j} &= u_{eq}^{\lambda} - b_c^{\lambda-1} k^{\lambda} \cdot isat(s^{\lambda}) \\ j &= 1,2,3,4 \end{aligned} \qquad \text{Eq.(41)}$$

where u_r : Yaw control input, u_v: Side slip control input u_{RI}: Rollover prevention control input, $u_{\lambda j}$: Longitudinal slip control input.

The obtained braking control inputs are applied according to the priority sequences of the braking control (wheel slip control, rollover prevention, side-slip control, yaw control), which is superior to CDC control application focusing on providing the ride comfort and the stable maneuver for the driver. Especially when we need the multi wheel braking, (ex: one wheel braking is not enough to control the vehicle) the necessary braking forces are

allocated at the additionally applied wheel.

4. STANDARD TEST AND WORST-CASE DYNAMIC EVALUTION

4.1 Standard test procedure

The performance of vehicles is frequently assessed by government agencies through well-defined standard tests. The test results are then published through New Car Assessment Programs, which has become a critical factor in consumer purchase decisions. In the US, rollover propensity is assessed through a 5-star rating system, which is based on static stability factor plus a correction based on fishhook test. The fishhook maneuver is selected by National Highway Transportation Administration (NHTSA) based on objectivity, repeatability, performability and discriminatory capability (21). Starting from the late 1990's, electronic stability control (ESC) systems quickly penetrate the market as an important active safety device. Car companies soon realize ESC is a relatively cheap way to improve the rollover star-rating of a SUV or light trucks. Instead of redesigning the vehicle chassis or weight distributions, ESC can be calibrated to affect vehicle handling and roll behaviors to boost the vehicle star rating.

NHTSA now faces a new and difficult problem: design

a simple, repeatable and reliable way to assess the performance of vehicles with smart chassis control systems. The problem is analogous to assessing the learning of students. Traditional "standard test" procedure is akin to announcing the exam questions ahead of time, and then trying to assess learning by grading the exam papers. Is it possible some "students" may do a great job answering the exam questions but otherwise learn very little about the rest if the course material? With "students" armed with advanced chassis control systems which can be easily tuned for any pre-announced standard test, the teacher (NHTSA) needs to find a revolution way to assess learning (safety performance).

The new testing method, we believe, needs to have three major characteristics: 1) The test cannot be one-size-fit-all. Instead, it needs to create customized test maneuvers for each vehicle; 2) The test needs to be simulation based, instead of experiment-based; and 3) The test needs to be based on comprehensive and rich test maneuvers; instead of relying on a handful of test maneuvers. These three characteristics are discussed separately in the following.

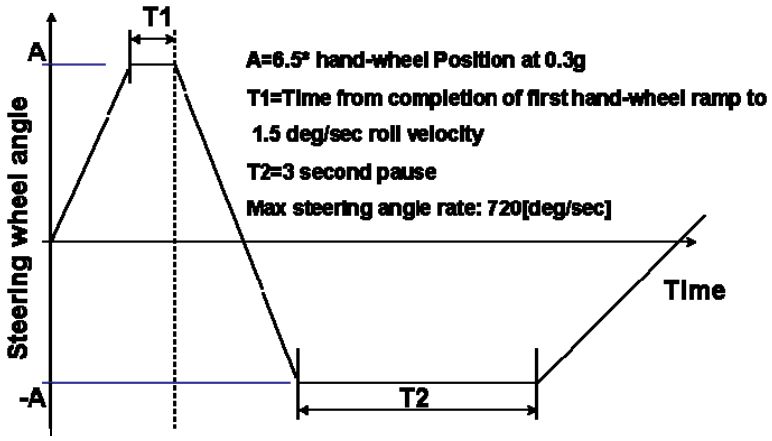

Fig. 8 NHTSA Fishhook tests for rollover

NHTSA started to move away from one-size-fit-all toward customized tests in recent years. As an example, Fig/8 shows the fishhook test maneuver defined by NHTSA for vehicle rollover propensity test. The hand-wheel steering magnitude 'A', and dwell time 'T1' are selected based on vehicle response and thus are different for each vehicle. This customization is necessary to ensure the test is somewhat normalized, and vehicles with low steering ratio or high performance tires are not penalized inadvertently. We believe more customization is necessary, to thoroughly assess the performance of smart control systems.

The current standard test practice also faces another major hurdle: experimental evaluations are, by nature, expensive, time-consuming and low repeatability because of the large number of uncontrolled variables and parameters such as tire wear and road friction.

4.2 Worst-case dynamic evaluation (WCDE)

The worst-case dynamic evaluation (WCDE) process, we believe, is a good alternative to the current experiments-based evaluation process for future vehicles, especially when they are equipped with active safety devices. The WCDE method is a simulation-based evaluation process that identifies weaknesses of a vehicle through extensive numerical search. The simulation-based approach eliminates the effect of human uncertainties. In addition, it allows a wide variety of scenarios, including those that are not feasible or too costly in field testing. Through extensive numerical search, WCDE challenges the vehicle with a large set of severe maneuvers and is a valuable asset in the development of active safety systems.

Mathematically, WCDE can be formulated as a trajectory optimization problem, which searches for the worst-possible driver's maneuvers that maximize a cost function, e.g., the 2-norm of vehicle roll angle through the optimization horizon. WCDE for ground vehicles and their control system had been attempted (36)(37). The focus of (36) was rollover and jackknifing of articulated vehicles using the worst-case evaluation methodology. In (37), various optimization methods such as direct method and indirect method were investigated and compared for WCDE applications.

The numerical machine of WCDE must be able to accommodate problems with one or more of three features: (i) nonlinear problems with complex numerical subroutines (e.g., CarSim, Adams, etc.); (ii) Problems with equality and/or inequality constraints; and (iii) performance index in non-accumulated form (e.g infinity norm). In addition, based on our past experience, the Dynamic Programming method, which ensures global optimality, is not practical for high-dimension dynamic systems due to the curse of dimensionality. Based on all these considerations, we choose the Sequential Quadratic Programming (SQP) method which is a local search method but is very efficient even for high-dimensional problem due to its rich development history.

The WCDE problem is set up as follows. The time horizon is discretized into grid points

$$t_0 = \tau_1 < \ldots < \tau_{N-1} < \tau_N = t_f \qquad \text{Eq.(42)}$$

where t_0 : intial time t_f : final time . The disturbance (e.g., steering wheel angle) at these discrete time grid points, $\mathbf{w}_{sw}$, are design variables to be solved for the optimization problem but the applied input is smoothed through interpolation (see Figure 9)

$$\mathbf{w}_{sw} = [w_{sw}^1, w_{sw}^2, \ldots, w_{sw}^{N-1}, w_{sw}^N] \qquad \text{Eq.(43)}$$

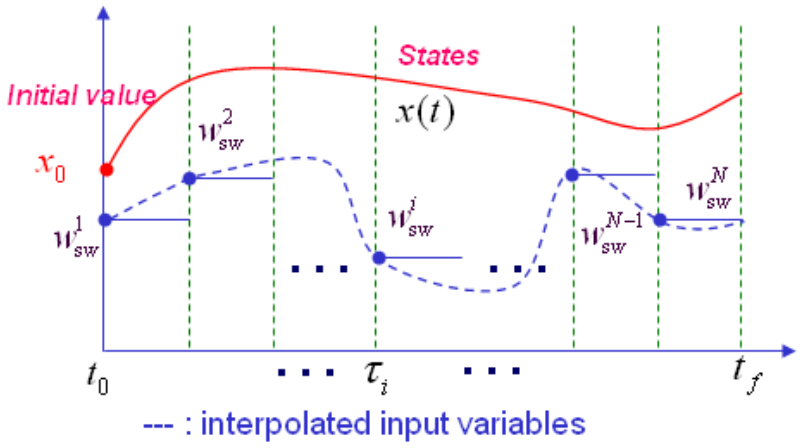

Fig. 9 WCDE problem setup

After surveying various methods, two numerical methods based on Mesh Adaptive Direct Searching (MADS) and Sequential Quadratic Programming (SQP) are selected (26). The MADS algorithm is a generalization of the class of Generalized Pattern Search (GPS) algorithms, a derivative-free method (28). The SQP method has been widely applied to many optimization problems (26)(27) and efficient softwares are available. However, both methods are local search methods and thus global optimality cannot be guaranteed. Therefore, it is critical to provide a rich set of initial guess of disturbance inputs, and both numerical methods will be used to find local optimum.

The major components of WCDE program are a constraint block and an initial point generation block. In these blocks, constraints such as magnitude saturation and rate limits are imposed. The initial point generation is

the most critical part of WCDE. Since both numerical methods only search locally, smart initial points that are rich and "bad enough" are critical for reaching an array of local optimal that truly reflect the safety performance. The generation of initial points is explained in details in the next section.

4.3. Generation of initial points

A common practice in generating initial points for local search methods such as SQP is to start form pseudo-random points. The idea is to cover the high dimensionality of the disturbance inputs in a systematical way. The generated inputs, however, will have certain level of randomness for richness. Some of the initial points used in our WCDE program will be generated in this pseudo-random fashion. However, we put more emphasis on another generation method—to leverage existing standard test, engineering practice and controls theory. Adoption of common testing maneuvers developed by vehicle safety research group such as NHTSA and University of Michigan Transportation Research Institute (UMTRI) are very appropriate. In addition, linear systems analysis, e.g., worst allowable persistent bounded disturbance (WAPBD) (25) also provides useful insight into disturbance input generation. This concept generates

worst-case input based on impulse response of linear time invariant (LTI) system. The procedure is described in Fig. 10. First, $g(t)$, the impulse response due to steering input is obtained. The response is trimmed at 3% steady-state error and the time span, T is determined. The worst persistent disturbance, $w_0(t,T)$ for $t \in [0,\mathrm{T}]$ is then obtained from $w_0(t,T) = \mathrm{sign}\{g(T-t)\}$. Assuming that the maximum steering value is $\delta_{\max}$, then a good initial point is $\delta_{\max} \cdot sign\{g(T-t)\}$.

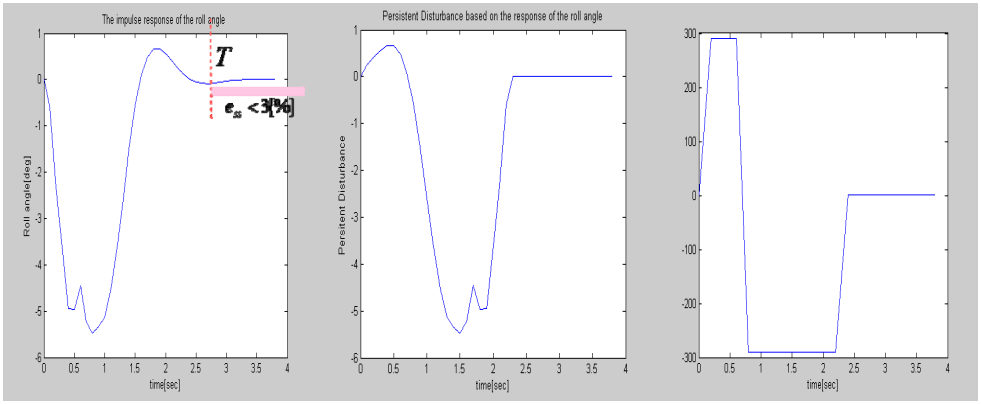

$$g(t) \quad \Rightarrow \quad w_0(t,T) = g(T-t) \Rightarrow \quad \delta_{\max} \cdot sign\{g(T-t)\}$$

Fig. 10 The initial point obtained from the impulse-response based WAPBD approach.

In addition to the WAPBD method, initial guess is also generated based on J-turn, fish-hook, fish-hook-with-dwell, UMTRI drastic maneuver, sinusoidal steering, and double lane-change. Search for local optimal around these commonly used testing maneuvers, as well as a set of pseudo-random initial conditions provide rich and customized search needed to provide rigorous

evaluations.

Despite of the fact both SQP and MADS are local-search methods, if large number of iterations is allowed, both methods may find local optimum that is quite different from the initial guess. One such example is illustrated below. In this example, the cost function to be minimized is selected to be $J = 1000 / |\phi_{\max}|^2$. From the initial condition using WAPBD explained in the above, both MADS and SQP methods are invoked. The maximum steering angle and steering rate are limited to 290[deg] and 1000[deg/s] based on NHTSA Fishhook test standard in Fig. 11.

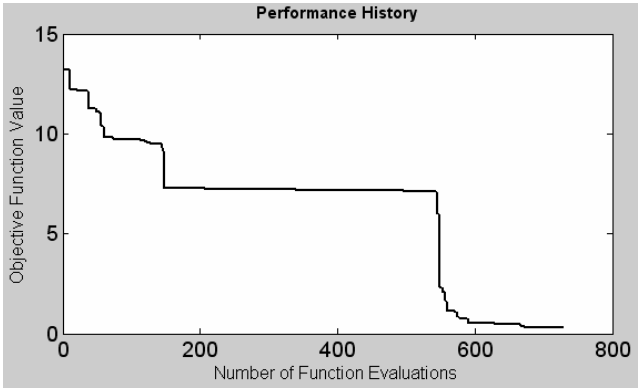

Fig. 12 MADS searching history $J = 1000 / |\phi|^2$

The searching history of the MADS method is shown in Fig. 12. It can be seen that the solution may be stuck at a certain cost function value for extended number of iterations before it suddenly break loose and find a better optimum point. This is typical of local search

methods, which demonstrates the need to allow large numbers of iterations.

	Iteration Number	Evaluation Function	Convergence Tolerance	Final Cost function
SQP	74	2019	0.001	0.31
MADS	349	729	0.001	0.31

Table 1. WCDE searching results

Both SQP and MADS methods were able to cause rollover, under the same initial condition. Detailed evaluation results are shown in Table 1. The performance of the two solutions is the same (J=0.31) despite of the fact the steering angle and vehicle roll motions are different (see Fig. 13). This indicates that they converge to different local minimum, both of which might be of interest in understanding the performance of the vehicle ICC system.

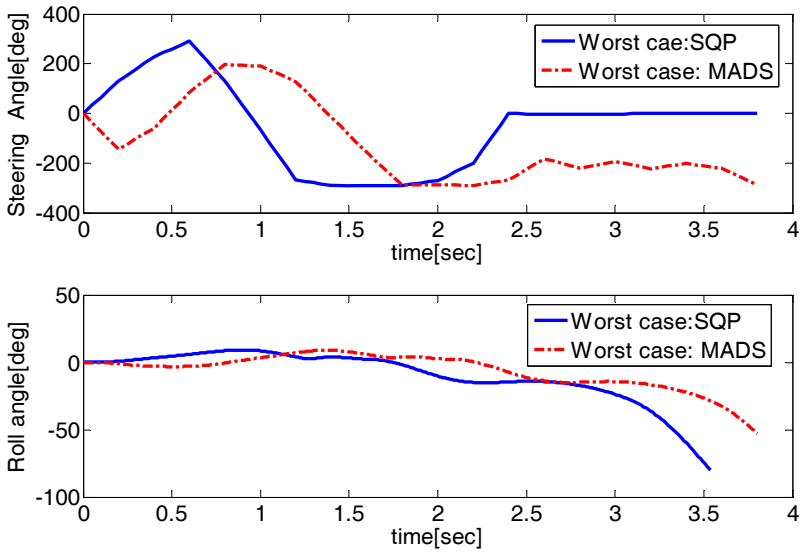

Fig. 13 Worst case maneuver result from SQP & MADS $u_x = 82[kph], \mu = 0.9$

The effectiveness of the obtained worst-case

maneuver (from SQP) is compared against a standard rollover test, the NHTSA Fishhook test. As shown in Fig. 14, It can be seen that the vehicle rolls over under the WCDE steering but not under the standard fishhook test. What is even more interesting is that we are able to repeat the same process and achieves rollover even when the initial vehicle speed is 10kph lower than that of the fishhook test (see Fig. 14).

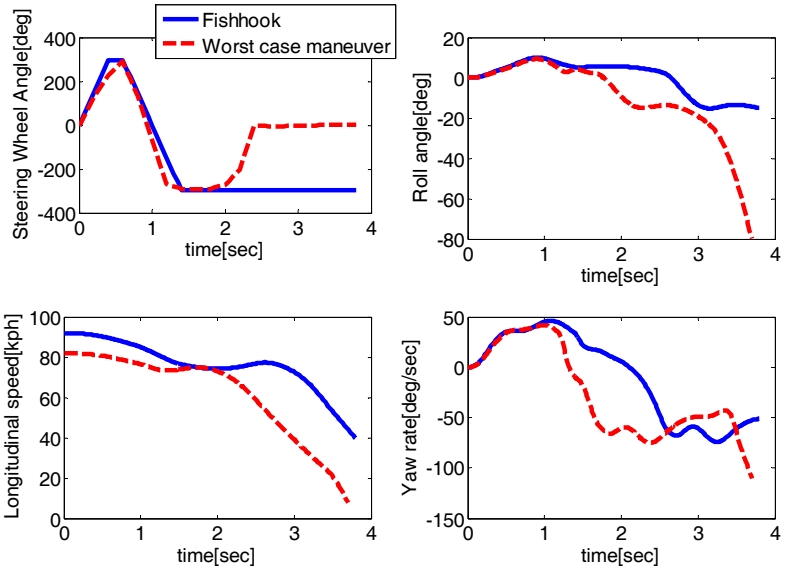

Fig. 14 Comparison simulation between standard Fishhook and the worst-case maneuver for rollover

5. SIMULATION RESULTS

In this section, two sets of simulations and one summary table are presented. The purpose of these simulations is to demonstrate how the developed WCDE procedure can be used to assess the performance of the ICC

system developed in Section 3.

The simulations are all based on the CarSim SUV vehicle model and the ICC system, if used, is calibrated based on this target vehicle. The first simulation is based on a double lane-change maneuver on low-μ surface, which is a "closed-loop" test using the MacAdam preview driver model. The purpose of this simulation is to illustrate the effect of ICC interacting with a human driver.

It can be seen from Fig. 14 that the driver's steering action is of much lower magnitude compared to that of the ICC-off case. In fact, since the vehicle speed is relatively high (85kph), the ICC-off case hits the road friction saturation bound and the vehicle spins out. The loss of vehicle stability is evident from the steep drop of vehicle speed. The driver of the ICC-off vehicle tries to counter steer but fails to stabilize the vehicle.

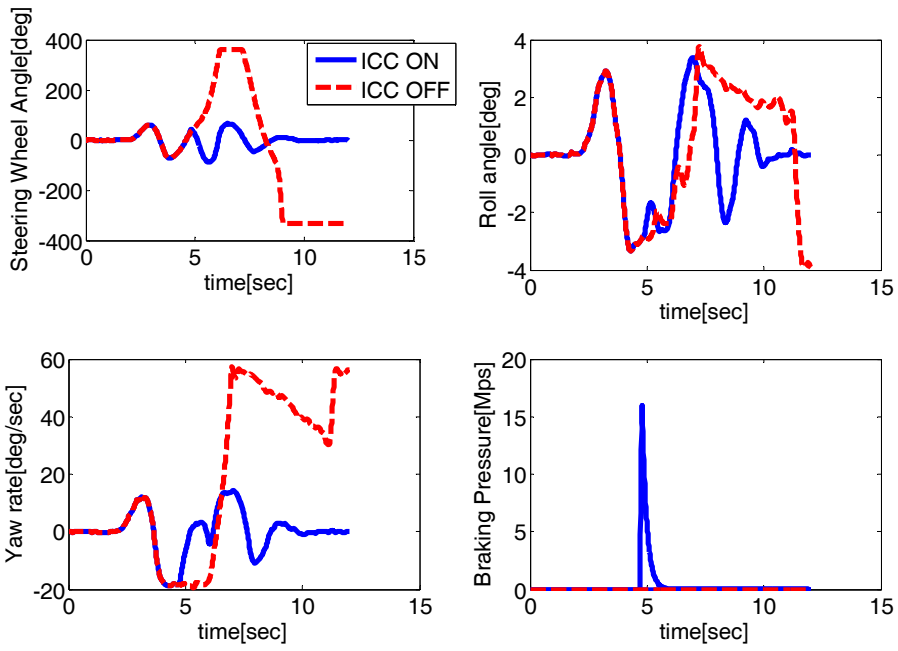

Fig. 15 Simulation results, Double lane change at $u_x = 85[kph]$, μ= 0.37

In Fig. 15, the worst-case maneuver from WAPBD-based initial point and SQP search in section 4.3 5was simulated on a high-μ road surface. The ICC-off vehicle rolls over while the ICC-on vehicle does not.

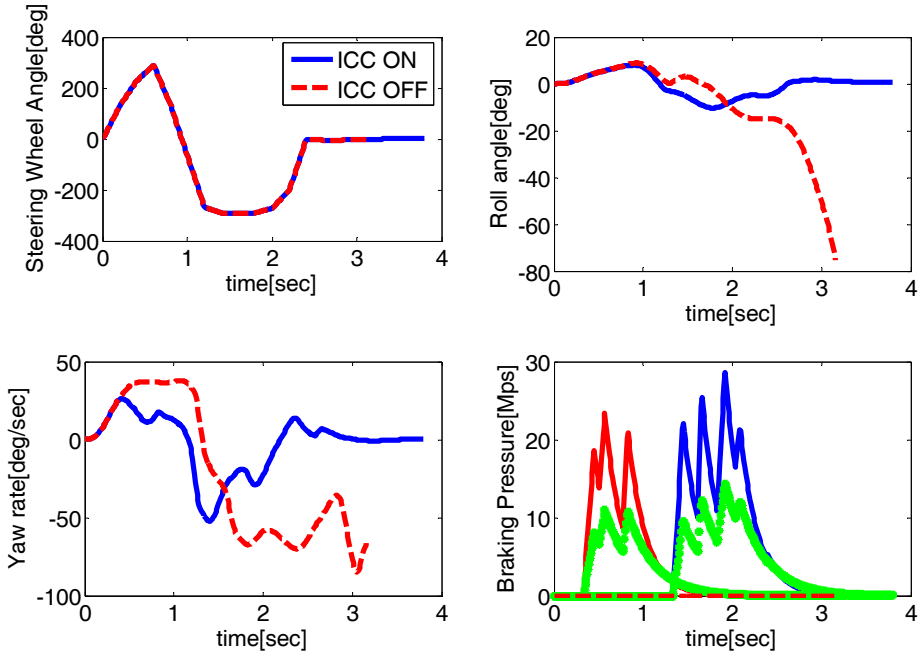

Fig. 16 Simulation Results, WCDE @ $u_x = 85[kph]$, μ= 0.9

Speed [kph]			80	100	120	140
Max Roll angle [deg]	WCDE	ICC ON	6.1	6.6	7.9	13.7
		ICC OFF	*Rollover*	*Rollover*	*Rollover*	*Rollover*
	Standard Test (ICC OFF)		15.3	*Rollover*	*9.8 (Spin-out)*	*10.4 (Spin-out)*

Table.2 Evaluation of ICC rollover prevention via standard test simulation and WCDE

$\mu = 0.9$

Table.2 is an important result obtained from the WCDE evaluation process. The cost function to be minimized is the same as the one used in Section 4, aiming to generate large roll motions. The results of WCDE are obtained by 10 initial point cases including standard test maneuvers, the resonance characteristics analysis, WAPBD,

etc. The SQP and MADS algorithms are then used to find local optimum. The result with the highest roll angle is then reported in table 2. For the "standard test" row, simulation results from the NHTSA fishhook test and NHTSA sine-dwell test are obtained and the highest roll angle is reported. When ICC is turned off, WCDE identified steering inputs that result in rollover for the target vehicle under all vehicle speeds. For standard tests, the vehicle might rollover or spin-out. In other words, the standard maneuvers are selected a priori, and may not be the best choice in terms of assessing vehicle rollover performance. The performance of the developed ICC is able to achieve consistently lower roll angle, in comparison with the ICC-off case. The results confirm that the ICC is tuned properly, from the worst-case sense. If any of the ICC-on case shows higher roll angle than ICC-off case, it will indicate a serious problem—the control-on case should never be worse-off than the no-control case under any circumstances. This required condition can be easily assessed through the WCDE process, but not traditional standard test process.

6. CONCLUSION

The development of a vehicle model with an integrated chassis control system and the evaluation of its

performance based on a worst-case dynamic evaluation process are reported in this paper.

The developed simple vehicle model acaptures the vehicle lateral-yaw-roll motions as well as the tire friction ellipse behavior. It was found to be accurate enough for ICC design purposes. The Integrated Chassis Control (ICC) system studied in this paper includes an electronic stability Control sub-system and a semi-active suspension sub-system. The ICC system is designed considering ride control, lateral motion control, yaw control, side-slip control, rollover prevention control and wheel slip control. The sliding mode control technique is used for the servo-loop design of ESC for guaranteed robustness.

The simulation based Worst-Case Dynamic Evaluation (WCDE) evaluation procedure is an optimization method which aims to find worst possible disturbance (e.g., driver's steering input) for defined vehicle motion. Because of the high system dimension, two local search methods, Sequential Quadratic Programming (SQP) and Mesh Adaptive Direct Searching (MADS) are used. Due to the local-search nature of these two methods, it is critical to provide good and rich starting points. A set of initial points, compiled from common practice used in the automotive field testing, plus procedures motivated by control theories are suggested. The worst-case evaluation

process is described and example results in assessing rollover performance of a vehicle with and without ICC are used to demonstrate the design process.

56. CONCLUSION

The development of a vehicle model with an integrated chassis control system and the evaluation of its performance based on a worst-case dynamic evaluation process are reported in this paper.

The developed simple vehicle model is applied for controller design and basic system analysis including evaluation process based on its modeling accuracy with minimal complexity. ICC controller model is composed by organizing based on safety priorities sequences the respective functionalities module such ride control, lateral motion control, yaw control, side-slip control, rollover prevention control and wheel slip control that stability focusing chassis control systems, CDC and ESC include . Sliding mode technique using 3 DOF vehicle model based on linearized tire ellipse model allows a compact and adaptive servo-loop control design of ESC, which is based on the vehicle parameters.

The novel simulation based evaluation procedure, WCDE, which is designed by vehicle model with control system, the optimization method and an initial point

generation, provided a systematic approach to validate the performance of the developed ICC system. From the worst-case study defined by rollover, feasibility of WCDE is approved by finding the failure mode the vehicle standard test can't detect. And based on this approved procedure the performance of the developed ICC model for SUV vehicle is verified in the various speed zones.

In an era when active control system for ground-vehicle and complex evaluation process continues to proliferate, the worst-case dynamic evaluation procedure is the next step for a customized evaluation approach via computer simulation.

REFERENCES

(1) Tim Gordon, Mark Howell and Felipe Brandao, "Integrated Control Methodologies for Road Vehicles", Vehicle System Dynamics 2003, Vol. 40, Nos. 1-3, pp. 157-190.

(2) A.T.van Zanten., "Bosch ESP System:5 Years of Experience", SAE Congress, SAE Paper No. 2000-01-1633, 2000.

(3) W. Ma and H. Peng, "A Worst-Case Evaluation Method for Dynamic Systems," ASME J. of Dynamic Systems, Measurement and Control, Vol.121, No.2, June 1999, pp.191-199.

(4) Cem Unsal and Pushikin Kachroo, “Sliding Mode Measurement Feedback Control for Antilock Braking Systems”, IEEE Transaction on control systems technology, Vol. 7, No. 2, March 1999.

(5) Bjorn Johansson, “Un-tripped SUV Rollover Detection and Prevention”, Department of Automatic Control Lund Institute of Technology February 2004. ISSN 0280-5316 ISRN LUTFD2/TFRT 5718 SE.

(6) Guenther, D.A. & Heydinger, G.J., “Vehicle dynamics modeling for the National Advanced Driving Simulator of a 1997 Jeep Cherokee”, SAE Paper No. 1999-01-0121.

(7) Hanlong Yang and Louis Yizhang Liu “A Robust Active Suspension Controller with Rollover prevention”, SAE Technical Paper 2003-01-0959.

(8) Jihan Ryu and J. Christian Gerdes “Estimation of Vehicle Roll and Road Bank Angle”, Proceeding of the 2004 American Control Conference Boston, Massachusetts, June 30-July 2, 2004.

(9) Jean-Jacques E.Slotine and Weiping Li “Applied Nonlinear Control”. pp. 276-307 ISBN 013-040890-5

(10) Agrawal, S.K. & Fabien, B.C., “Optimization of dynamic systems”, Kluwer Academic Publishers, Netherlands, 1999.

(11) Allen, R.W., Rosenthal, T.J & Szostak, H.T.,

"Analytical modeling of driver response in crash avoidance maneuvering –Volume 1: Technical Background", NHTSA, DOT HS 807 270, April, 1988.

(12) Athans, M. & Falb, P.L., "Optimal control", McGraw-Hill, New York, 1966.

(13) Aldo Sorniotti and Mauro Velardocchia., "Hardware-In-the-Loop(HIL) Testing of ESP Commercial Hydraulic and Implementation of New Control Strategies", 22nd Annual Brake Colloquium & Exhibition , SAE Paper No. 2004-01-2770, 2004.

(14) Guenther, D.A. & Heydinger, G.J., "Vehicle dynamics modeling for the National Advanced Driving Simulator of a 1997 Jeep Cherokee", SAE Paper No. 1999-01-0121.

(15) Sage, A.P. & White , C.C., "Optimum systems control", Prentice-Hall, 1997.

(16) A. Y. Ungoren and H. Peng, "Evaluation of Vehicle Dynamic Control for Rollover Prevention," International Journal of Automotive Technology, Vol.5, No.2, June 2004, pp.115-122.

(17) Wielenga, T. J., "A method for reducing on-road rollovers – Anti-rollover braking", SAE Congress, SAE Paper No. 1999-01-0123, 1999.

(18) Cem Unsal and Pushikin Kachroo, "Sliding Mode Measurement Feedback Control for Antilock Braking

Systems", IEEE Transaction on control systems technology, VOL. 7, NO. 2, March 1999

(19) Hanlong Yang and Louis Yizhang Liu "A Robust Active Suspension Controller with Rollover prevention", SAE Technical Paper 2003-01-0959.

(20) Jihan Ryu and J. Christian Gerdes "Estimation of Vehicle Roll and Road Bank Angle", Proceeding of the 2004 American Control Conference Boston, Massachusetts June 30-July 2, 2004.

(21) NHTSA "NHTSA Phase IV Final Report" October 2002

(22) Jasbir S. Arora., "Introduction to Optimum Design" , McGraw-Hill international editions

(23) Panos Y. Papalambros and Douglass J.Wilde ., "Principle of Optimal design," modeling and computation

(24) Jean-Jacques E. Slotine and Weiping Li, Applied Nonlinear Control, ISBN 013-040890-5

(25) Jayasuriya, S. "On the Determination of the worst allowable persistent bounded disturbance for a system with constraints" ASME Journal of Dynamic Systems, Measurement and Control Vol. 117,pp 126-133 JUNE 1995

(26) John T. Betts "Survey of Numerical Methods for Trajectory Optimization", JOURNAL OF GUIDANCE, CONTROL, AND DYNAMICS Vol. 21, No. 2,

March–April 1998

(27) Christof Buskens ; Helmut Maurer “SQP-methods for solving optimal control problems with control and state constraints: adjoint variables, sensitivity analysis and real-time control” Journal of Computational and Applied Mathematics, 120, pp 85-108, 2000

(28) Charles Audet and J.E. Dennis JR. “Mesh Adaptive Direct Search Algorithm for Constrained Optimization” SIAM Journal on Optimization archive, Volume 17, Issue 1, pp 188-217, 2006.

(29) Ian J. Fialho and Tryphon T. Georgiou, Senior Member, IEEE “Worst Case Analysis of Nonlinear Systems” IEEE Transactions on Automatic Control, Vol. 44, No. 6, JUNE 1999

(30) Frank L. Lewis, “Applied Optimal Control and Estimation” Prentice-Hall International Editions

(31) Zoltán K. Nagy and Richard D. Braatz, “Worst-Case and Distributional Robustness Analysis of Finite-Time Control Trajectories for Nonlinear Distributed Parameter Systems” IEEE Transactions on Control System Technology, VOL. 11, NO. 5, Sep 2003

(32) Wayne W. LU, Gary J. Balas and E. Bruce Lee “Linear quadratic performance with worst case disturbance rejection.” INT. J. Control, Vol. 73, NO. 16 2000

(33) G. E. Ivanov "Saddle Point for Differential Games With Strongly Convex-Concave Integrand" Mathematical Noten, Vol. 62, No. 5, 1997

(34) Arthur E. Bryson, Jr., and Yu-Chi Ho, Applied Optimal Control, 1969.

(35) National Highway Traffic Safety Administration (NHTSA), DOT. Final rule. "Federal Motor Vehicle Safety Standards Electronic Stability Control Systems Controls and Displays" 2007.

(36) Ma, W.H., "Worst-case evaluation methods for vehicles and vehicles control systems", PhD. Dissertation, Dept. of Mechanical Engineering and Applied Mechanics, University of Michigan, Ann Arbor, 1998.

(37) Ungoren, A.Y., "Worst-case evaluation methods for rollover prevention system", PhD. Dissertation, Dept. of Mechanical Engineering and Applied Mechanics, University of Michigan, Ann Arbor, 2003.

(38) Moritz Diehl, "Adjoint Based SQP Methods for Fast Real-Time Optimal Control," University of Heidelberg, Germany SIOPT Stockholm, May 18, 2005.

(39) Karnopp, D. C. "Active damping in road vehicle suspension systems". Veh. System Dynamics, Nov 1982.